

Calculation of optical-waveguide grating characteristics using Green's functions and the Dyson's equation

Lars Rindorf

*COM•DTU, Department of Communications, Optics and Materials,
Technical University of Denmark, DK-2800 Kgs. Lyngby, Denmark*

Niels Asger Mortensen

*MIC, Department of Micro and Nanotechnology, NanoDTU,
Technical University of Denmark, DK-2800 Kgs. Lyngby, Denmark*

We present a method for calculating the transmission spectra, dispersion, and time delay characteristics of optical-waveguide gratings based on Green's functions and Dyson's equation. Starting from the wave equation for transverse electric modes we show that the method can solve exactly both the problems of coupling of counter-propagating waves (Bragg gratings) and co-propagating waves (long-period gratings). In both cases the method applies for gratings with arbitrary dielectric modulation, including all kinds of chirp and apodisation and possibly also imperfections in the dielectric modulation profile of the grating. Numerically, the method scales as $\mathcal{O}(N)$ where N is the number of points used to discretize the grating along the propagation axis. We consider optical fiber gratings although the method applies to all 1D optical waveguide gratings including high-index contrast gratings and 1D photonic crystals.

PACS numbers: 42.79.Dj, 42.25.-P, 42.25.-Bs

I. INTRODUCTION

Spectral properties of optical fiber waveguide gratings [1, 2] have typically been addressed with coupled-mode theory (CMT) [3, 4, 5, 6]. The theory relies on entities with a clear physical interpretation and despite its approximations (slowly varying amplitude, small index modulation, and synchronous approximations) it has proved successful in accounting for the behavior of long-period gratings (LPGs) and Bragg gratings (BGs) with uniform dielectric modulation, i.e. a dielectric modulation of the grating with constant period and peak value. Over the years corrections to CMT for non-uniform gratings as well as more general solutions have been addressed in a number of papers including Refs. 7, 8, 9, 10, 11, 12.

Others have addressed the problem of gratings with arbitrary dielectric modulations through iterative solution of integral equations in inverse scattering methods, such as the Gel'fand–Levitan–Marchenko coupled equations [13, 14]. The iterative solution of the integral equations scales as $\mathcal{O}(N^3)$, where N is the number of points along the propagation axis, and does not always converge for strong Bragg gratings. The convergence problem can be remedied by using the approximate layer-peeling algorithm [15] which is based on a combination of transfer matrices [16] and a differential scattering formulation [17]. Originating in geophysics the layer-peeling algorithm divides a non uniform grating into a number of uniform segments. Numerically the method scales as $\mathcal{O}(N^2)$.

In this paper we offer a Green's function method (GFM) based on the solution of the *Dyson's* integral equation that is exact for coupling of co-propagating transverse electric waves as well as counter-propagating

transverse electric waves. The numerical implementation scales as $\mathcal{O}(N)$. Our calculation of the Green's function formally relies on methods from quantum mechanics and the many-body theory of condensed matter systems, see e.g. Refs. 18, 19. Interpreting the Green's function as a space(-time) propagator immediately provides us a link to the transmission and reflection properties of finite-length gratings and thus forms a physical interpretation of the Green's function.

The GFM thus offer an exact integral method, which also may be formulated in terms of transfer matrices. Furthermore, perturbative calculations may be readily be carried out with the Dyson's equation. To demonstrate the method we calculate spectra, time delay, and dispersion characteristics for uniform, as well as apodised and chirped fiber gratings.

The Green's functions and the Dyson's equation have previously been used in electromagnetical systems for a variety of problems (see Ref. 20 and references therein), among those finite size 2D photonic crystals [21, 22, 23].

The paper is organised as following. In Sec. II we describe the problem of optical waveguide gratings. In Sec. III we describe the problem in terms Maxwells equations. In Secs. IV,V we introduce the Green's function formalism and the Dyson's equation. In Sec. VI we apply the theory to long-period gratings and in Sec. VII to Bragg gratings. In Secs. VIII and IX discussions and conclusions are provided.

II. OPTICAL WAVEGUIDE GRATINGS

The waveguide grating is a scattering region introduced in the waveguide and is effectively equivalent to a one dimensional finite size photonic crystal. Wave-

uides support a number of guided modes; one or two fundamental modes and an infinite number of higher order modes. All modes have a forward and a backward propagating part. In the so-called *long-period grating* different forward propagating modes couple at a resonant frequency. Forward scattering involves a very small momentum transfer $\delta\beta = k\Delta n^{\text{eff}}$ where $k = \omega/c = 2\pi/\lambda$ is the free-space wavenumber and Δn^{eff} is the difference in effective indices of the resonant modes involved. Since $\delta\beta\Lambda_G \sim 1$ at resonance, the period Λ_G of such a grating is necessarily long, hence its name. In Bragg gratings the forward and backward propagating parts of the same mode couple involving a large momentum transfer $\delta\beta = 2\beta = 2kn^{\text{eff}}$ and thus Bragg gratings necessarily have a short grating period Λ_G .

The dielectric modulation seen in Fig. 1 can be perfectly periodic with Λ_G (uniform grating) or can be quasi-periodic (non-uniform grating). It is possible to alter the spectral characteristics of a grating by using *apodisation* and *chirp* in the dielectric modulation Ref. [24]. Such techniques have made gratings widely used as highly selective bandpass filters [25], dispersion compensators and pulse compressors [26, 27] and optical sensors [28]. With apodisation the magnitude of the peak dielectric modulation varies across the length of the grating.

With chirp the period of the grating varies across the grating. Apodisation and chirp, however, may also appear as an unwanted error in an intended uniform grating due to fabrication imperfections.

Side-lobe suppression can be done by an apodisation known as raised-Gaussian apodisation [29] where the dielectric modulation has a Gaussian envelope.

In a linear chirp the grating period varies as $\Lambda_G(z) = \Lambda_G(1 + \frac{c_1}{2} \frac{z}{L})$ where c_1 is the chirp parameter and L is the length of the grating. Apodisation can be visualised as segments of uniform gratings that are concatenated. The spectra are different due to different peak dielectric modulation, but share the same resonance wavelength. A chirped grating can be visualised as the concatenation of uniform grating segments with different grating periods.

III. GENERAL FORMALISM

In the following we consider temporal harmonic solutions to Maxwell's equations with electrical fields of the form $\mathbf{E}(\mathbf{r}, t) = \mathbf{E}_\omega(\mathbf{r})e^{-i\omega t}$, with the subscript ω indicating the frequency dependence. The electrical field is a solution to a vectorial wave equation, which has the form of a generalised eigenvalue problem [20, 30],

$$\nabla \times \nabla \times \mathbf{E}_\omega(\mathbf{r}) - k^2 \boldsymbol{\varepsilon}_r(\mathbf{r}_\perp) \mathbf{E}_\omega(\mathbf{r}) - k^2 \boldsymbol{\varepsilon}_G(\mathbf{r}) \mathbf{E}_\omega(\mathbf{r}) = 0, \quad (1)$$

where the dielectric functions, $\boldsymbol{\varepsilon}$, are 3×3 dielectric tensors. \mathbf{r}_\perp is the coordinate vector orthogonal to the axis of the fiber which we define to be parallel with the z-axis. The subscript ‘r’ refers to what we will call the reference system, which is the bare fiber without any grating. $\boldsymbol{\varepsilon}_r$

is thus translational invariant along the z-axis. The subscript ‘G’ refers to the changes in the dielectric function induced by the grating. The grating begins at z_i and ends at z_f and $\boldsymbol{\varepsilon}_G(\mathbf{r})$ is thus zero outside this interval. Usually $\boldsymbol{\varepsilon}_G(\mathbf{r})$ is denoted as $\delta\boldsymbol{\varepsilon}_G(\mathbf{r})$ because it is assumed that it is small, but here we use the former notation to emphasise that the presented theory is formally valid for any dielectric profile including high-index contrast profiles since Eq. (1) is completely general. In the following $\boldsymbol{\varepsilon}_G(\mathbf{r})$ is referred to as the dielectric modulation and we will for simplicity omit the subscript on \mathbf{E}_ω .

In order to solve Eq. (1) for a general $\boldsymbol{\varepsilon}_G$ we will use a Hilbert function space spanned by the monochromatic (fixed k) eigensolutions to the reference system in Eq. (1)

$$\mathbf{E}_m^{(0)}(\mathbf{r}) = \mathbf{E}_m^{(0)}(\mathbf{r}_\perp) e^{i\beta_m z}, \quad (2)$$

where β_m is the propagation constant of the mode m . For the inner product we have $\langle E_m^{(0)} | E_n^{(0)} \rangle = \int d\mathbf{r} \mathbf{E}_m^{(0)\dagger}(\mathbf{r}) \cdot \mathbf{E}_n^{(0)}(\mathbf{r})$, where \dagger is the Hermitian conjugate (transpose and complex conjugate) of the field vector. We choose the eigenmode basis $\{E_m^{(0)}\}_{m=1}^M$ to be orthonormal, $\langle E_m^{(0)} | \hat{\varepsilon}_r | E_n^{(0)} \rangle = (\frac{\beta_m}{k})^2 \delta_{mn}$, where δ is the Kronecker delta function. This orthonormalisation follows from the fact that Eq. (1) is a generalised eigenvalue problem. Any linear operator \hat{O} on a Hilbert space of finite dimension can be represented by a matrix acting on a state vector as $\hat{O} = \sum_{mn} O_{mn} |E_m^{(0)}\rangle \langle E_n^{(0)}|$, where \hat{O} has matrix elements $O_{mn} = \int d\mathbf{r} \mathbf{E}_m^{(0)\dagger}(\mathbf{r}) \mathbf{O}(\mathbf{r}) \mathbf{E}_n^{(0)}(\mathbf{r})$.

For transverse electric modes, dielectric tensors with $\varepsilon_{xz} = \varepsilon_{zx} = \varepsilon_{yz} = \varepsilon_{zy} = 0$, and it is possible to integrate out the transverse degrees of freedom in Eq. (1) to obtain

$$\frac{d^2}{dz^2} |E\rangle + k^2 \hat{\varepsilon}_r |E\rangle + k^2 \hat{\varepsilon}_G(z) |E\rangle = 0, \quad (3)$$

where $|E\rangle$ is a linear combination of eigenmodes with scalar coefficients, i.e. (state) vector in the eigenmode basis $\{E_m^{(0)}\}_{m=1}^M$. We have thus transformed the fully vectorial eigenvalue problem of Eq. (1) into a scalar eigenvalue problem given by Eq. (3) in the Hilbert function space spanned by the fully vectorial eigenmodes.

IV. GREEN'S FUNCTIONS

In the following we address Eq. (3) with the aid of Green's functions which will in turn provide us with insight in the transmission and reflection properties of the grating.

A. Solution with Dyson's equation

Let $G^{(0)}$ be the zero-order Green's function solution to the eigenvalue equation, Eq. (3) with $\boldsymbol{\varepsilon}_G = 0$. This has

the analytical solution

$$iG_{mn}^{(0)}(z, z') = \delta_{mn} \frac{e^{i\beta_m |z-z'|}}{2\beta_m}. \quad (4)$$

The zero-order Green's function only depends on $z' - z$ in agreement with the assumption of translational invariance of the reference system. The zero-order Green's function can conveniently be split into a spatial forward propagating and a backward propagation part

$$\begin{aligned} & \theta(z - z') iG_{+,mm}^{(0)}(z, z') + \theta(z' - z) iG_{-,mm}^{(0)}(z, z') \\ &= \theta(z - z') \frac{e^{i\beta_m(z-z')}}{2\beta_m} + \theta(z' - z) \frac{e^{-i\beta_m(z-z')}}{2\beta_m}. \end{aligned} \quad (5)$$

The subscripts '+' and '-' refer to the forward and backward propagating part of the Green's function, respectively, and θ is Heaviside's stepfunction. We also note that $G_+^{(0)}$ and $G_-^{(0)}$ have the convenient mathematical property that they each split in their variables: $e^{\pm i\beta_m(z-z')} = e^{\pm i\beta_m z} e^{\mp i\beta_m z'}$. In terms of $G^{(0)}$ the Green's function solution to the full grating problem Eq. (3) is given by the *Dyson's equation* [20]

$$\begin{aligned} i\mathbf{G}(z, z') &= i\mathbf{G}^{(0)}(z, z') \\ &- i \int_{z_i}^{z_f} dz'' i\mathbf{G}^{(0)}(z, z'') k^2 \hat{\varepsilon}_G(z'') i\mathbf{G}(z'', z'). \end{aligned} \quad (6)$$

The integration interval is changed to $[z_i, z_f]$ since ε_G is zero outside this interval.

B. Physical properties of the Green's functions

The transmission and reflections properties may be described in a scattering basis formulation where ingoing and outgoing modes are related to each other by a scattering matrix

$$\mathbf{S} = \begin{pmatrix} \mathbf{r} & \mathbf{t}' \\ \mathbf{t} & \mathbf{r}' \end{pmatrix}. \quad (7)$$

Here, t_{mn} is the transmission amplitude for forward scattering (left-to-right direction) from mode n to mode m and r_{mn} is the reflection amplitude for back-scattering (left-to-left direction) from mode n to mode m . Likewise, t' and r' are amplitudes for the opposite directions. We restrict ourselves to lossless media for which \mathbf{S} is unitary and symmetric so that $\mathbf{t}' = -\mathbf{t}^\dagger$, $\mathbf{r}' = \mathbf{r}^\dagger$, and $\mathbf{1} = \mathbf{r}^\dagger \mathbf{r} + \mathbf{t}^\dagger \mathbf{t}$. The Green's function is naturally interpreted as a propagator for field amplitudes and the full Green's function may be related to the bare Green's function via [19]

$$iG_{mn}(z_f, z_i) = t_{mn} \frac{e^{i(\beta_m z_f - \beta_n z_i)}}{2\sqrt{\beta_m \beta_n}} \quad (8a)$$

$$iG_{mn}(z_i, z_i) = r_{mn} \frac{e^{i(\beta_m - \beta_n)z_i}}{2\sqrt{\beta_m \beta_n}} \quad (8b)$$

and the transmission and reflection probabilities become

$$T_{mn} = |t_{mn}|^2 = 2^2 \beta_m \beta_n |iG_{mn}(z_f, z_i)|^2, \quad (9a)$$

$$R_{mn} = |r_{mn}|^2 = 2^2 \beta_m \beta_n |iG_{mn}(z_i, z_i)|^2. \quad (9b)$$

The group delays of the transmission and reflection are given by the phase of the amplitude coefficients, t_{mn} and r_{mn} . The group delay for the scattering $n \rightarrow m$ is given by

$$\tau_{mn} = \arg(t_{mn}), \quad (10)$$

where $\arg(x)$ is the argument of the complex number of x . For the group delay of the reflection scattering similar arguments hold and the group delay may be obtained by substituting t_{mn} with r_{mn} in Eq. (10). The dispersion, D , of the $n \rightarrow m$ scattering is defined as the derivative of the group delay with respect to wavelength

$$D_{mn} \equiv \frac{d\tau_{mn}}{d\lambda}. \quad (11)$$

V. THE INTERMEDIATE GREEN'S FUNCTION

The dielectric modulation of the grating not only causes the different modes to coupled, but also the individual modes to change. This phenomenon is also referred to as *self-coupling* and has the physical interpretation that the grating causes the individual propagation constant of a mode ($\beta_m = n_m^{\text{eff}} k$) to change slightly. Self-coupling is typically of second importance to cross-mode coupling in fiber gratings and it can in many instances be ignored. However, we can at no cost incorporate it in the free forward and backward Green's function propagators and we refer to these new propagators \tilde{G}_\pm as the *intermediate Green's functions*. By this trick we eventually end up with a Dyson's equation for the full Green's function with a particular simple structure. To see this we split $\hat{\varepsilon}_G$ into two Hermitian operators: a self-coupling operator (s), which is diagonal in its indices, and a cross (x) coupling operator which is purely off-diagonal:

$$\hat{\varepsilon}_G(z) = \hat{\varepsilon}^s(z) + \hat{\varepsilon}^x(z) \quad (12a)$$

$$\varepsilon_{mn}^s(z) \equiv \delta_{mn} \varepsilon_{G,mm}(z) \quad (12b)$$

$$\varepsilon_{mn}^x(z) \equiv \varepsilon_{G,mn}(z) - \varepsilon_{mn}^s(z) \quad (12c)$$

The diagonal, self-coupling component, ε^s , is often referred to as the 'DC' component and the cross coupling component, ε^x , as the 'AC' component in analogy with electric engineering. We first consider the forward Green's function. To zero order in the self-coupling the intermediate Green's function equals the free Green's function, $\tilde{G}_+^{(0)}(z', z) = G_+^{(0)}(z', z)$. Iterating Dyson's equation and keeping terms to linear order in $\hat{\varepsilon}^s$ gives the correspond-

ing contribution to the intermediate Green's function

$$\begin{aligned} & -i \int_z^{z'} dz'' i\mathbf{G}_+^{(0)}(z', z'') k^2 \hat{\varepsilon}^s(z'') i\mathbf{G}_+^{(0)}(z'', z) \\ & = i\mathbf{G}_+^{(0)}(z', z) \frac{-ik^2}{2\beta} \int_z^{z'} dz'' \hat{\varepsilon}^s(z''). \end{aligned} \quad (13)$$

With the operator

$$\Delta\beta(z', z) \cdot (z' - z) \equiv \frac{k^2}{2\beta} \int_z^{z'} dz'' \hat{\varepsilon}^s(z''), \quad (14)$$

we may solve Dyson's equation, Eq. (6), straightforwardly to any order. One might wonder why we chose to define a function as in Eq. (14). This definition has the advantages that the left hand side is distributive in z and z' , $\Delta\beta(z', z) \cdot (z' - z) = \Delta\beta(z', z'') \cdot (z' - z'') + \Delta\beta(z'', z) \cdot (z'' - z)$, and if the equation is divided by $z' - z$, then it can be seen that $\Delta\beta_{mm}$, is proportional to an average of ε_G over $z' - z$. We will use these properties in the following. For the backward propagating intermediate Green's function the analysis above may be repeated. Using the distributive property of $\Delta\beta$ and introducing

$$\tilde{\beta}(z)z \equiv \beta z + \Delta\beta(z, z_i) \cdot (z - z_i) \quad (15)$$

we may write the forward and backward propagating intermediate Green's functions as

$$\theta(z - z') i\tilde{\mathbf{G}}_+(z, z') = \theta(z - z') \frac{e^{i\tilde{\beta}(z)z} e^{-i\tilde{\beta}(z')z'}}{2\beta}, \quad (16a)$$

$$\theta(z' - z) i\tilde{\mathbf{G}}_-(z, z') = \theta(z' - z) \frac{e^{-i\tilde{\beta}(z)z} e^{i\tilde{\beta}(z')z'}}{2\beta}, \quad (16b)$$

which are diagonal matrices in their mode indices. The Dyson equation (6) may be rewritten in terms of the intermediate Green's functions and the cross coupling operator

$$\begin{aligned} i\mathbf{G}(z', z) & = i\tilde{\mathbf{G}}(z', z) \\ & - i \int_{z_i}^{z_f} dz'' i\tilde{\mathbf{G}}(z', z'') k^2 \hat{\varepsilon}^x(z'') i\mathbf{G}(z'', z). \end{aligned} \quad (17)$$

A. Numerical evaluation of Dyson's equation

The Dyson's equation (17) describes a system of $M \times M$ coupled equations. Due to the fact that the matrix $i\tilde{\mathbf{G}}$ is diagonal in its mode indices the different matrix columns of $i\mathbf{G}$ are not coupled to each other, and the Dyson's equation constitute M problems of size M instead of a single problem of size $M \times M$. If only a single electric mode is incident on the grating (as is often, but not always, the case) only a single column of the matrix Dyson's equation needs to be solved. For large M and N this gives a significant reduction in time and memory consumption.

The matrix Dyson's equation (17) may be solved by simple iteration by inserting $\tilde{\mathbf{G}}$ on the position of \mathbf{G} on the right hand side of the equation to obtain $\sum_{\alpha=0}^1 i\mathbf{G}^{(\alpha)}(z, z')$ on the left hand side. This in turn may be inserted to find $\sum_{\alpha=0}^2 i\mathbf{G}^{(\alpha)}(z, z')$. Such an iteration may be continued until any order. In this work we evaluated Dyson's equation with the discrete dipole approximation [31]. In the approximation the scattering interval $[z_i, z_f]$ is discretised into N cells. Each cell is assumed small enough that the variations of the electric field $\mathbf{E}(z)$ and the dielectric modulation $\varepsilon_G(z)$ are negligible within the cell.

The numerical task of evaluating a single iteration with Eq. (17) generally scales as N^2 where N is the number of cells on the discretised z grid. However due to the distributive property of the forward and backward propagating intermediate Green's functions shown in Eqs. (16a,16b), the calculation scales as N .

VI. COPROPAGATING WAVES - LONG-PERIOD GRATINGS

In a LPG the power of an incident core mode is coupled into a forward propagating cladding mode which has a different, smaller propagation constant, β , but the same frequency ω . The cladding modes are slightly lossy causing the mode power of the cladding mode to slowly dissipate into the environment of the waveguide. Thus in practice the total energy transmitted through the waveguide is reduced by the amount of energy transmitted into the cladding mode. Physically, the cladding mode losses are small over the length of a grating and may be neglected in the calculations.

A. Resonance condition

To analyse the resonance, we may neglect higher order contributions than first order in $\hat{\varepsilon}^x$ (but retain all orders in $\hat{\varepsilon}^s$) to the total Green's function

$$\begin{aligned} i\mathbf{G}(z_f, z_i) & = i\mathbf{G}^{(0)}(z_f, z_i) + i\mathbf{G}^{(1)}(z_f, z_i) \\ & = \frac{e^{-i\tilde{\beta}(z_f)z_f}}{\sqrt{2\beta}} \left(\mathbf{1} - i\boldsymbol{\kappa}(z_f, z_i)(z_f - z_i) \right) \frac{e^{i\tilde{\beta}(z_i)z_i}}{\sqrt{2\beta}}, \end{aligned} \quad (18)$$

where the cross-coupling function, $\boldsymbol{\kappa}$, is defined as

$$\begin{aligned} \boldsymbol{\kappa}_{mn}(z', z) \cdot (z' - z) & = \\ & \frac{k^2}{2\sqrt{\beta_m\beta_n}} \int_z^{z'} dz'' e^{-i(\tilde{\beta}_m(z'') - \tilde{\beta}_n(z''))z''} \varepsilon_{mn}^x(z''). \end{aligned} \quad (19)$$

We can thus estimate the resonant wavelength by finding the maximum of $|\boldsymbol{\kappa}_{mn}|$ with respect to the wavelength.

For uniform gratings with constant period and strength we may rearrange the integrand of the expression as [37]

$$e^{-i(\tilde{\beta}_m(z) - \tilde{\beta}_n(z))z} \varepsilon_{mn}^x(z) = e^{-i(\overline{\tilde{\beta}_m(z)} - \overline{\tilde{\beta}_n(z)})z} \times e^{-i(\tilde{\beta}_m(z) - \overline{\tilde{\beta}_m(z)} - \tilde{\beta}_n(z) + \overline{\tilde{\beta}_n(z)})z} \varepsilon_{mn}^x(z). \quad (20)$$

The middle factor on the right hand side of Eq. (20) does not have a different period than $\varepsilon_{mn}^x(z)$. The self-coupling thus changes the resonant frequency from $8\beta_m - \beta_n = \frac{2\pi}{\Lambda_G}$ to an average $\overline{\tilde{\beta}_m(z)} - \overline{\tilde{\beta}_n(z)} = \frac{2\pi}{\Lambda_G}$ in the limit $\frac{z_f - z_i}{\Lambda_G} \rightarrow \infty$. This result is the same as that of the *synchronous approximation* used in CMT [5, 6] which arises from different arguments.

B. Numerical solution of Dyson's equation

We consider a system of a pair of coupling modes: a core mode and a cladding mode. Only the forward propagating Green's functions need to be considered as the coupling to the backward propagating modes is far from resonance and is negligible. The use of only forward propagating Green's functions alters the integration limits in the Dyson's equation, Eq. (17), due to the step function in the forward propagating intermediate Green's function, Eq. (16a). We consider a system where only a single core mode is incident on the grating and thus need only to solve the first column of the matrix Dyson's equation, Eq. (17)

$$\begin{bmatrix} i\tilde{G}_{\text{co,co}}(z, z_i) \\ i\tilde{G}_{\text{cl,co}}(z, z_i) \end{bmatrix} = \begin{bmatrix} i\tilde{G}_{\text{co}}(z, z_i) \\ 0 \end{bmatrix} - ik^2 \int_{z_i}^z dz' \begin{bmatrix} i\tilde{G}_{\text{co}}(z, z') & 0 \\ 0 & i\tilde{G}_{\text{cl}}(z, z') \end{bmatrix} \begin{bmatrix} 0 & \varepsilon_{\text{co,cl}}^x(z') \\ \varepsilon_{\text{cl,co}}^x(z') & 0 \end{bmatrix} \begin{bmatrix} iG_{\text{co,co}}(z', z_i) \\ iG_{\text{cl,co}}(z', z_i) \end{bmatrix}, \quad (21)$$

where we have set the notation as $\tilde{G}_{\text{co}}(z, z_i) = \tilde{G}_{11}(z, z_i)$ and $\tilde{G}_{\text{cl}}(z, z_i) = \tilde{G}_{22}(z, z_i)$. The contributions to the total Green's function from zero to second order in $\hat{\varepsilon}^x$ can be seen in Fig. 2. Numerically, we can improve the discrete dipole approximation employed in this paper by rescaling the top and bottom row by $1/\tilde{G}_{\text{co}}(z, z_i)$ and $1/\tilde{G}_{\text{cl}}(z, z_i)$, respectively, since the rescaled total Green's function varies more slowly within the cells than the original Green's function due to $\Lambda_G \gg \lambda$ for LPGs. To solve the system we use the simple iteration method discussed in Sec. V A. The iteration may be continued until the desired accuracy is reached. In this work we iterate until the root mean square of the residue between two consecutive iterations is less than 10^{-12} . The dielectric modulation is chosen as a uniform modulation $\varepsilon_G(\mathbf{r}) = \Delta\varepsilon(\mathbf{r}_\perp) \frac{1}{2}(1 - \cos(\frac{2\pi}{\Lambda_G}z))$. We model a typical fiber LPG with resonance tentatively at $\lambda \simeq 1550\text{nm}$ with the peak dielectric change $\Delta\varepsilon = 2.5 \times 10^{-3}$, a grating period of $\Lambda_G = 500\mu\text{m}$, and a difference in the effective indices of $n_{\text{co}}^{\text{eff}} - n_{\text{cl}}^{\text{eff}} = \frac{1550\text{nm}}{\Lambda_G}$. The difference in the effective indices is assumed constant with respect to the wavelength. The elements of the operator $\hat{\varepsilon}$, are given by $\frac{\varepsilon_{\text{co,co}}^s(\mathbf{r})}{\varepsilon_G(\mathbf{r})} = 0.60$, $\frac{\varepsilon_{\text{cl,cl}}^s(\mathbf{r})}{\varepsilon_G(\mathbf{r})} = 0.20$, and $\frac{\varepsilon_{\text{co,cl}}^x(\mathbf{r})}{\varepsilon_G(\mathbf{r})} = \frac{\varepsilon_{\text{cl,co}}^x(\mathbf{r})}{\varepsilon_G(\mathbf{r})} = 0.10$. Finally, the dielectric constant of silica is $\varepsilon_{\text{si}} = 2.10$.

With the given parameters we model the spectra of the grating with four different lengths $L = \frac{\pi}{10\kappa} = 8\text{mm}$, $\frac{\pi}{3\kappa} = 13.5\text{mm}$, $\frac{\pi}{2\kappa} = 20\text{mm}$, $\frac{\pi}{\kappa} = 40\text{mm}$ corresponding to 16, 27, 40, and 80 grating periods, respectively, and κ is given by the maximum of Eq. (19) with respect to wavelength.

The LPG couples the core mode power into the cladding mode with cosine-like amplitude behavior as

seen in Fig. 3. In passing we note that the LPG effectively corresponds to a rotation of the state vector in the Hilbert space spanned by $\{\mathbf{E}_{\text{co}}, \mathbf{E}_{\text{cl}}\}$. The $\frac{\pi}{2}$ rotation seen in the bottom left figure in Fig. 4 can be made into a π rotation seen in the bottom right figure in Fig. 4 by doubling the length of the grating. The resonant wavelength found by Eq. (19) is 1615.7 nm. This includes the self-coupling of the modes which causes a considerable shift of the resonant wavelength of 65.7 nm. The time delay and the dispersion of the core transmission can be calculated with Eqs. (10,11) and is seen in Figs. 5, 6. The LPG has a low group delay and dispersion making it suitable as a dispersion-free wide-band rejection filter.

If the dielectric modulation has a Gaussian envelope the grating is said to be raised Gaussian apodised [29]. The so-called taper parameter which determines the strength of the apodisation is $g = \frac{1}{2}$. In Fig. 7 is shown the spectrum for a grating that is 40 mm long with 80 grating periods. The apodisation is seen to reduce the side-lobes seen in Fig. 4. We also model a linearly chirped grating with the chirp constant chosen as $c_1 = 0.005$. Thus the grating period varies 0.5% across the length. The number of grating periods is 40 corresponding to a total grating length of 20 mm and apart from the chirp the resulting spectrum would be identical to the one seen bottom left in Fig. 4. The spectrum of the chirped grating can be seen in Fig. 8. The 0.5% variation in the grating period is seen to have a clear effect on the spectrum. The side-lobes of the same magnitude as those of the uniform grating and the resonant wavelength is shifted to 1631.6 nm from 1615.7 nm even though the average grating period has remained the same.

VII. COUNTER-PROPAGATING WAVES - BRAGG GRATINGS

As explained in Sec. II BGs couple the counter-propagating part of the same mode. The coupling of the copropagating modes is so far from resonance that it is neglected. We will in the following suppress the mode subscript.

A. Resonance condition

Following the same line of arguments as in Sec. VI A we arrive at

$$\kappa(z', z) \cdot (z' - z) = \frac{k^2}{2\beta} \int_{z_i}^{z_f} dz'' e^{-i2\bar{\beta}(z'')z''} \varepsilon^x(z''). \quad (22)$$

$$\begin{bmatrix} i\tilde{G}_{+,+}(z, z_i) \\ i\tilde{G}_{-,+}(z, z_i) \end{bmatrix} = \begin{bmatrix} i\tilde{G}_+(z, z_i) \\ 0 \end{bmatrix} - ik^2 \begin{bmatrix} \int_{z_i}^z dz' i\tilde{G}_+(z, z') & 0 \\ 0 & \int_z^{z_f} dz' i\tilde{G}_-(z, z') \end{bmatrix} \begin{bmatrix} 0 & \varepsilon_{+, -}^x(z') \\ \varepsilon_{-, +}^x(z') & 0 \end{bmatrix} \begin{bmatrix} i\tilde{G}_{+,+}(z', z_i) \\ i\tilde{G}_{-,+}(z', z_i) \end{bmatrix}, \quad (23)$$

where we have abbreviated $\tilde{G}_+ = \tilde{G}_{+,+}$ and $\tilde{G}_- = \tilde{G}_{-,+}$. The equation (23) may be solved in the discrete dipole approximation by simple iteration as discussed in Sec. V A. The expressions obtained by simple iteration from zero order through second order can be seen in Fig. 9 in a diagrammatic representation. It is seen that a reflected wave has undergone an uneven number of interactions whereas the transmitted wave has undergone an even number of interactions. This fact is true for all orders of interactions.

The iteration may be continued until the desired accuracy is reached. In this report we iterate until the root mean square of the residue between two consecutive iterations is less than 10^{-12} . When simple iteration of Dyson's equation converges this may be met in less than 20 iterations. Simple iteration often diverges for strong BGs. For uniform gratings it is possible to analyze the divergence. We will not discuss this analysis in detail here, but only assert that simple iteration converges for uniform gratings when $|\kappa|L < \pi/2$ implying $T_{co,co} \gtrsim 0.16$. For stronger and non-uniform gratings Dyson's equation (23) may be solved as a self-consistency problem in $i\tilde{G}_{+,+}(z', z_i)$. In this paper we have employed a generalised minimum residue method for stronger gratings [32]. In our numerical algorithm the generalised minimum residue method automatically takes over if simple iteration of Dyson's equation diverges.

We choose the parameters of the gratings to closely resemble a standard fiber BG with resonance tentatively at $\lambda \simeq 1550\text{nm}$, leading to a grating period of $\Lambda_G = \frac{1550\text{nm}}{2} \frac{k}{\beta}$. The peak dielectric modulation is $\Delta\epsilon =$

This expression resembles Eq. (19) but has different integration limits due to the step function in Eq. (16b). For a uniform grating we may again conclude that self-coupling changes the resonance condition from $2\beta = \frac{2\pi}{\Lambda_G}$ to an average $2\bar{\beta}(z) = \frac{2\pi}{\Lambda_G}$ in the limit $\frac{z_f - z_i}{\Lambda_G} \rightarrow \infty$, which also is the result of the synchronous approximation used in CMT [5, 6].

B. Numerical solution of Dyson's equation

We will solve the Dyson's equation (17) by direct numerical solution. Since we consider a system where electric mode is incident from the left, we only have to evaluate the first column of the matrix Dyson's equation

2.5×10^{-3} , and the elements of the dielectric operator $\hat{\varepsilon}$ are given by $\frac{\varepsilon_{+,+}^s(\mathbf{r})}{\varepsilon_G(\mathbf{r})} = \frac{\varepsilon_{-,+}^s(\mathbf{r})}{\varepsilon_G(\mathbf{r})} = \frac{\varepsilon_{+,+}^x(\mathbf{r})}{\varepsilon_G(\mathbf{r})} = \frac{\varepsilon_{-,+}^x(\mathbf{r})}{\varepsilon_G(\mathbf{r})} = 0.50$. BGs with four different lengths are shown in Fig. 10. The length is given in the terms of the coupling constant at resonance, κ , given by Eq. (22). The lengths of the four gratings are 1.145mm, 2.290mm, 4.581mm, 9.161mm, for $\kappa L = 1/2, 1, 2, 4$, and with 2143, 4285, 8570, 17140, grating periods, respectively. Group delay and dispersion of the core transmission can be found using the Eqs. (10,11). The dispersion and delay for the transmission coefficient for the $\kappa L = 1$ and $\kappa L = 4$ are shown in Fig. 11 and Fig. 12, respectively.

If we use raised-Gaussian apodisation [29] with length $L = 9.161\text{mm}$ and the taper parameter, $g = 1/4$ we get the spectrum in Fig. 13. Apart from the apodisation the grating has the same parameters as the uniform grating shown bottom right in Fig. 10. The apodisation has removed the side lobes and ripples seen in spectrum of the uniform grating, but has lower reflection (higher transmission) at resonance. The group delay and dispersion are also smoother for the apodised grating as seen in Fig. 14.

Linear chirp has been incorporated in the grating seen in Fig. 15. The chirp parameter is chosen as $c_1 = 5 \times 10^{-5}$ and the length of the grating is 4.581mm. The group delay and dispersion of the transmission is seen in Fig. 16. It is seen that the chirp affects both the spectrum and the group delay and dispersion when comparing with a uniform grating.

VIII. DISCUSSION

The numerical results of GFM differ from the widely used CMY in two respects. The small oscillation seen in Fig. 3 does not occur in CMT, since it results from the second order derivative which is neglected in CMT. In GFM the oscillation occurs for both LPGs and BGs, but vanishes with decreasing coupling strength and averages out in general. CMT relies on a Fourier decomposition of the dielectric modulation. This is a very good approximation when the grating is uniform and has a high number of periods. An LPG usually have a modest number of periods compared with an BG, and the GFM spectra differ from CMT spectra in the side-lobes, while they coincide around the resonance. The GFM could therefore be applied for better apodisation of LPGs. BGs have a large number of periods, and thus CMT and GFM agree well for the uniform and the weakly apodised and chirped BGs presented in this report. However, BGs are being designed with increasing complex dielectric modulations to obtain extraordinary spectral and dispersive characteristics. The GFM may here be useful in the respect, that it does not divide the dielectric modulation into uniform segments, and therefore offers more freedom when designing the apodised dielectric modulation. The GFM could also be used to study the mechanisms of apodisation, which are still not completely understood [35].

The examples considered have all been fiber gratings. The GFM method is exact for transverse electric modes, but some optical fibers do not support these transverse modes. However the non-transverse part of a mode usually only holds a very small fraction of the total electrical field and contributes only negligible to the grating characteristics.

Although the presented theory is exact from the transverse electrical wave equation Eq. (1) the theory is in fact only exact within the basis set of the electric fields of the reference system (in finite element methods this is known as Galerkin error being zero). The electrical fields of the reference system may or may not describe the grating well. This is actually a feature in all grating theories and should not cause any worries, but some consideration

should be taken when applying the GFM to high-index contrast systems. A discussion of the variational error of the basis set can be found in [36].

The Green's functions and the Dyson's equation have here been used to model linear dielectric modulations. The theory can be adapted to a non-linear dielectric modulations, both local and non-local, for simulating harmonic generation, soliton dynamics and other non-linear effects. If a non-local dielectric modulation is used then powerful perturbative methods can be employed such as the Feynman diagrams used in many-body physics.

In Figs. 12, 5 it is seen that the group delay for both Bragg and long-period gratings is negative near resonance. This may seem conflicting with causality, but physically it is perfectly possible that the group velocity (pulse envelope velocity) is greater than the speed of light or even zero [33] causing negative time delays. However, numerical simulations indicate that negative group velocities are impossible in passive one-dimensional periodic media [34].

IX. CONCLUSION

A method for calculation of optical-waveguide gratings' optical characteristics based on Green's functions and the Dyson's equation has been presented. We have presented accurate spectra for long-period and both uniform and apodised BGs as well as the group delay and dispersion characteristics.

The GFM is exact for transverse electric modes for gratings with arbitrary dielectric modulations in both the long-period and the BG application. The method incorporates self-coupling in an exact analytic manner and also gives an exact resonance condition for gratings with arbitrary dielectric modulations. The GFM relies on iterative solution of integral equations which scales as $\mathcal{O}(N)$ which may be solved to within any given accuracy.

The GFM may also be useful in simulating non-linear problems or imperfect gratings with random mode scattering.

-
- [1] G. Meltz, W. W. Morey, and W. H. Glenn, *Opt. Lett.* **14** (15), 823 (1989).
 - [2] K. O. Hill and G. Meltz, *J. Lightwave Technol.* **15** (8), 1263 (1997).
 - [3] H. Kogelnik and C. Shank, *J. Appl. Phys.* **43**, 2327 (1972).
 - [4] A. Yariv, *IEEE J. Quant. Electron.* **QE-9**, 919 (1973).
 - [5] T. Erdogan, *J. Opt. Soc. Am. A* **14**, 1760 (1997).
 - [6] T. Erdogan, *J. Lightwave Technol.* **15**, 1277 (1997).
 - [7] J. E. Sipe, L. Poladian, and M. de Sterke, *J. Opt. Soc. Am. A* **11**, 1307 (1994).
 - [8] K. G. Sullivan and D. G. Hall, *Opt. Commun.* **118**, 509 (1995).
 - [9] L. Poladian, *Phys. Rev. E* **54**, 2963 (1996).
 - [10] V. M. N. Passaro, R. Diana, and M. N. Armenise, *J. Opt. Soc. Am. A* **19**, 1844 (2002).
 - [11] V. M. N. Passaro, R. Diana, and M. N. Armenise, *J. Opt. Soc. Am. A* **19**, 1855 (2002).
 - [12] L. A. Wellerbrophy and D. G. Hall, *J. Opt. Soc. Am. A* **2**, 863 (1985).
 - [13] E. Peral, J. Capmany, and J. Marti, *Electron. Lett.* **32**, 918 (1996).
 - [14] E. Peral, J. Capmany, and J. Martin, *IEEE J. Quantum Electron.* **32**, 2078 (1996).
 - [15] R. Feced, M. N. Zervas, and M. A. Muriel, *IEEE J. Quantum Electron.* **35**, 1105 (1999).

- [16] M. Yamada and K. Sakuda, *Appl. Opt.* **26**, 3474 (1987).
- [17] A. Bruckstein, B. Levy, and T. Kailath, *SIAM Journal on Applied Mathematics* **45**, 312 (1985).
- [18] A. L. Fetter and J. D. Walecka, *Quantum Theory of Many-Particle Systems* (McGraw-Hill, Inc., 1971).
- [19] H. Bruus and K. Flensberg, *Many-Body Quantum Theory in Condensed Matter Physics* (Oxford University Press, Oxford, 2004).
- [20] O. J. F. Martin, C. Girard, and A. Dereux, *Phys. Rev. Lett.* **74**, 526 (1995).
- [21] O. J. F. Martin, C. Girard, D. R. Smith, and S. Schultz, *Phys. Rev. Lett.* **82**, 315 (1999).
- [22] A. I. Rahachou and I. V. Zozoulenko, *Phys. Rev. B* **72**, 155117 (2005).
- [23] L.-M. Zhao, X.-H. Wang, B.-Y. Gu, and G.-Z. Yang, *Phys. Rev E* **72**, 026614 (2005).
- [24] P. S. Cross and H. Kogelnik, *Opt. Lett.* **1**, 43 (1977).
- [25] M. Ibsen, M. Durkin, M. Cole, and R. Laming, *IEEE Photonic Technol. Lett.* **10**, 842 (1998).
- [26] F. Ouellete, *Opt. Lett.* **12**, 847 (1987).
- [27] J. E. Roman and K. A. Winick, *IEEE J. Quantum Electron.* **29**, 975 (1993).
- [28] B. Lee, *Optical Fiber Technology* **9**, 57 (2003).
- [29] H. J. Deyerl, N. Plougmann, J. B. Jensen, F. Floreani, H. R. Sorensen, and M. Kristensen, *Appl. Opt.* **43** (17), 3513 (2004).
- [30] J. D. Joannopoulos, R. D. Meade, and J. N. Winn, *Photonic crystals: molding the flow of light* (Princeton University Press, Princeton, 1995).
- [31] B. T. Draine and P. J. Flatau, *J. Opt. Soc. Am. A* **11**, 1491 (1994).
- [32] URL <http://www.mathworks.com/>.
- [33] M. Mitchell and R. Y. Chiao, *American Journal of Physics* **66**, 14 (1998).
- [34] L. Poirier, R. I. Thompson, and A. Haché, *Opt. Com.* **250**, 258 (2005).
- [35] P. Minzioni and M. Tormen, *J. Lightwave Technol.* **24**, 605 (2006).
- [36] L. Rindorf and N. A. Mortensen, *Opt. Com.* **261**, 181 (2006).
- [37] Here we have defined the average of a function, f , as
$$\overline{f(z)} \equiv \frac{1}{z_f - z_i} \int_{z_i}^{z_f} dz f(z)$$
-

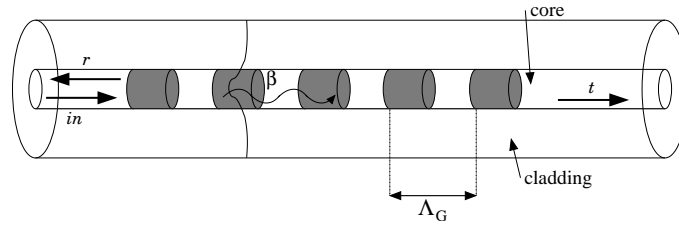


FIG. 1: An optical fiber waveguide with a grating consisting of a dielectric modulation in the core (grey area) with period Λ_G . The incident electric mode in with propagation constant β is partially reflected, (r), and partially transmitted (t) by the grating. No radial symmetry is assumed in the presented theory.

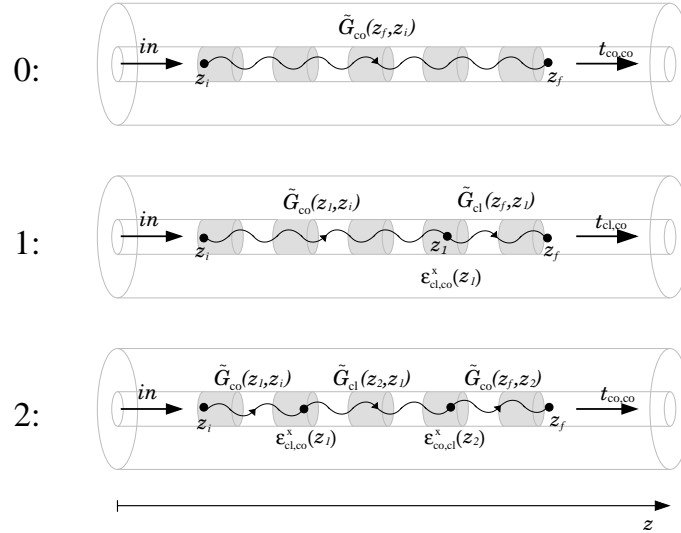


FIG. 2: Diagrammatic representation the zero to second order contributions to the total Green's function Eq. (21). An incident core mode interacts with a copropagating cladding mode through the dielectric modulation.

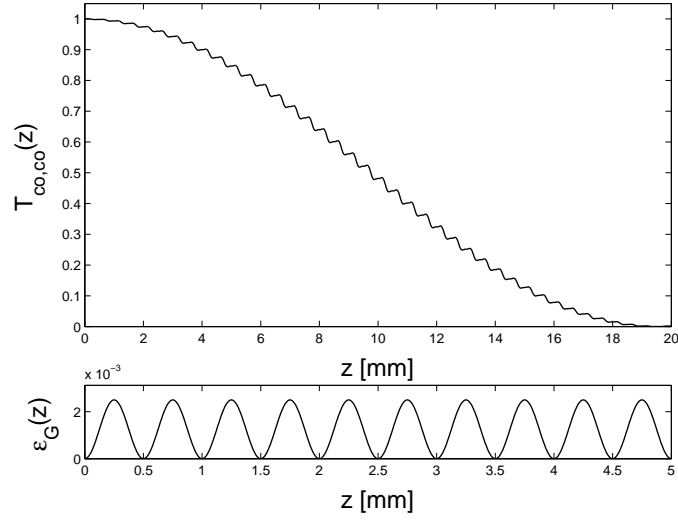


FIG. 3: Uniform LPG at the resonant wavelength. Top: The transmission of the core mode, T_{co} , as function of the grating length. Bottom: the uniform dielectric modulation of the grating.

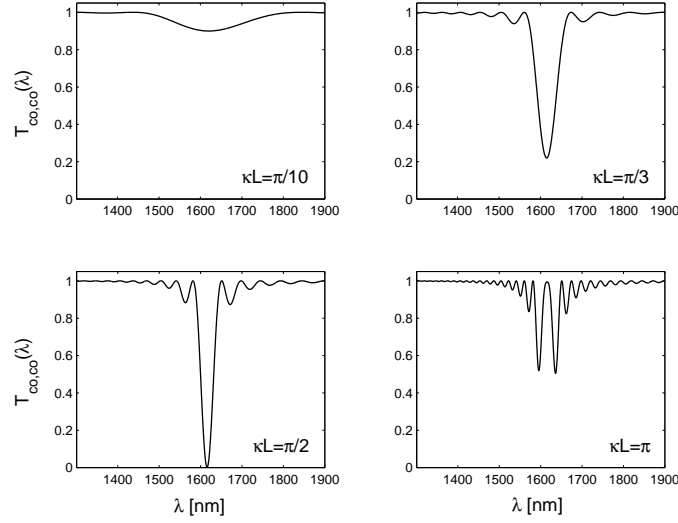


FIG. 4: Spectra of uniform LPGs with a uniform dielectric modulation (bottom in Fig. 3). The spectra is plot calculated for four different for grating lengths, $z_f - z_i = \frac{\pi}{10\kappa}, \frac{\pi}{3\kappa}, \frac{\pi}{2\kappa}, \frac{\pi}{\kappa}$ corresponding to 16, 27, 40, and 80 grating periods, respectively. At $\kappa L = \frac{\pi}{2}$ (bottom left) all core mode power is transferred into the cladding mode and back again into the core mode at $\kappa L = \pi$ (bottom right).

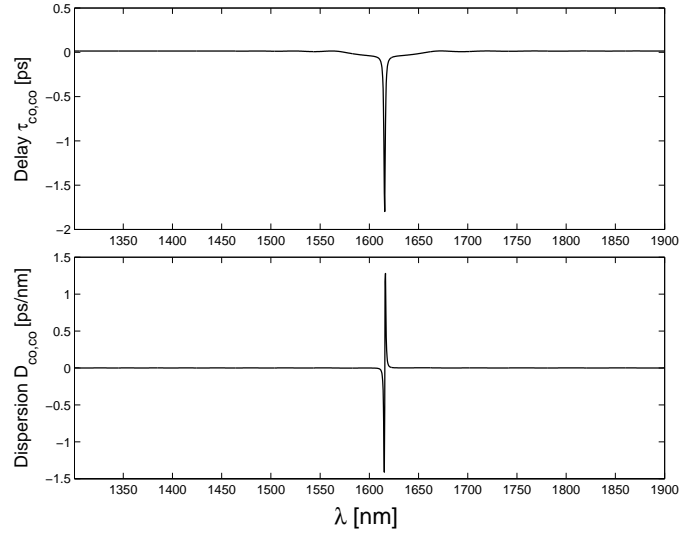


FIG. 5: Time delay and dispersion of the uniform long-period grating with length $z_f - z_i = \frac{\pi}{2\kappa}$. The corresponding spectrum is seen in the bottom left of Fig. 4.

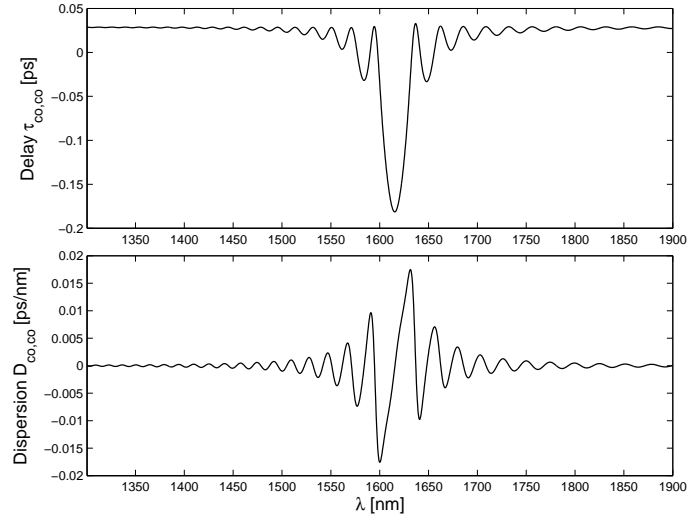


FIG. 6: Time delay and dispersion of the uniform long-period grating with length $z_f - z_i = \frac{\pi}{\kappa}$. The corresponding spectrum is seen in the bottom right of Fig. 4.

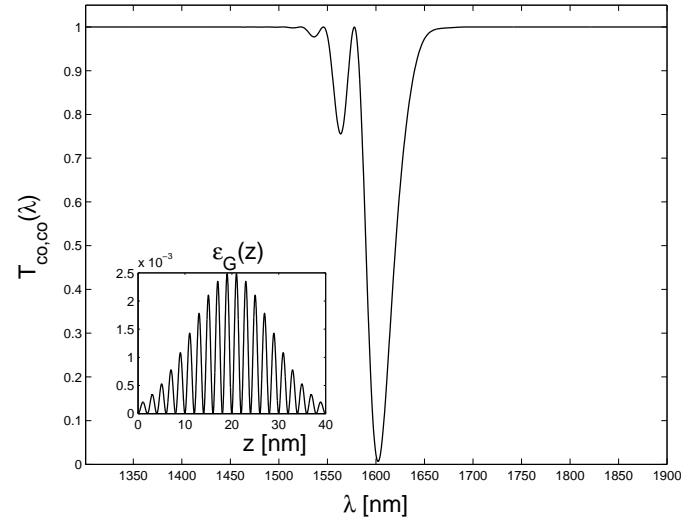


FIG. 7: Apodised LPG. The side-lobes seen in the bottom left of Fig. 4 have been reduced. Insert: a schematic view of the raised Gaussian apodised dielectric modulation. The grating period has been exaggerated with respect to the grating length for clarity.

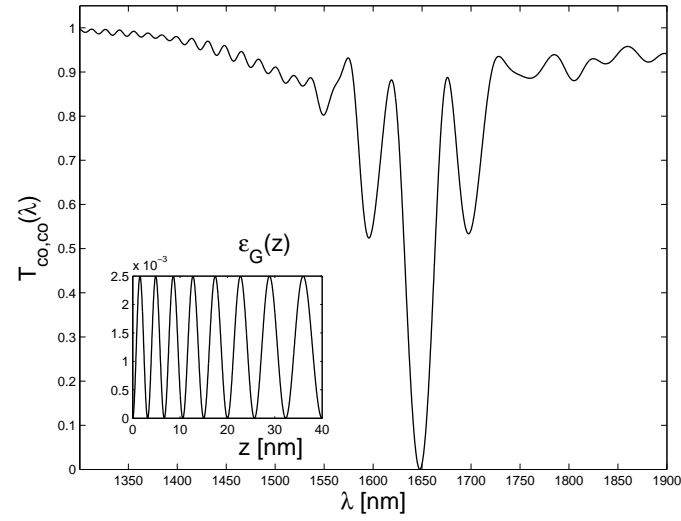


FIG. 8: Linearly chirped LPG. The side-lobes seen in the bottom left of Fig. 4 have been enhanced rather than reduced. Insert: a schematic view of the linearly chirped grating period of the dielectric modulation. The grating periods and the chirp have been exaggerated with respect to the grating length for clarity.

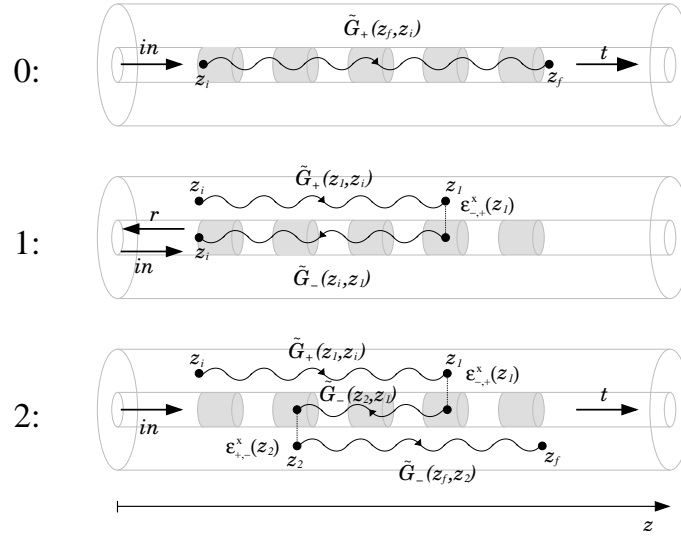


FIG. 9: Diagrammatic representation of the zero to second order contributions to the total Green's function Eq. (23) for a BG. An incident core mode interacts with its oppositely propagating counterpart through the dielectric modulation.

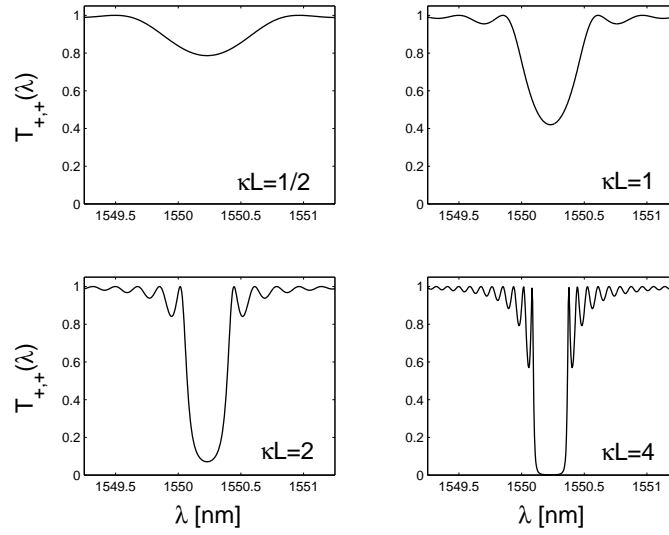


FIG. 10: Uniform BG spectra for four different lengths, $\kappa L = 1/2, 1, 2, 4$. The Bragg rejection band is emerging for increasing κL .

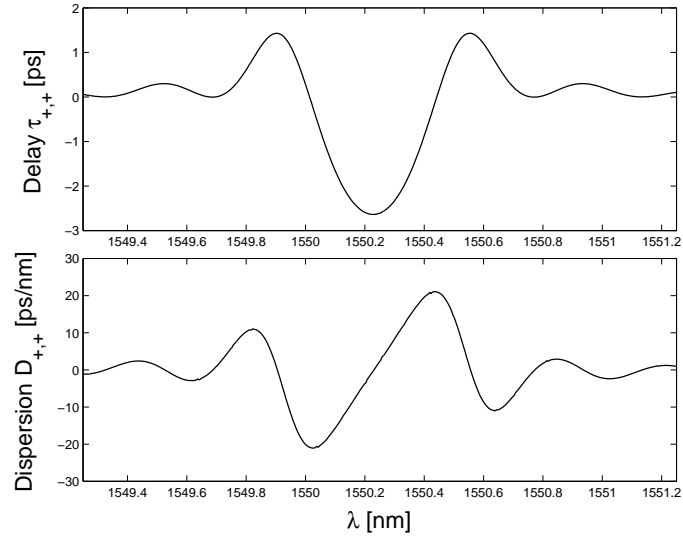


FIG. 11: Group delay and dispersion for the transmission coefficient of a uniform BG with $\kappa L = 1$. The corresponding spectrum is shown top right in Fig. 10.

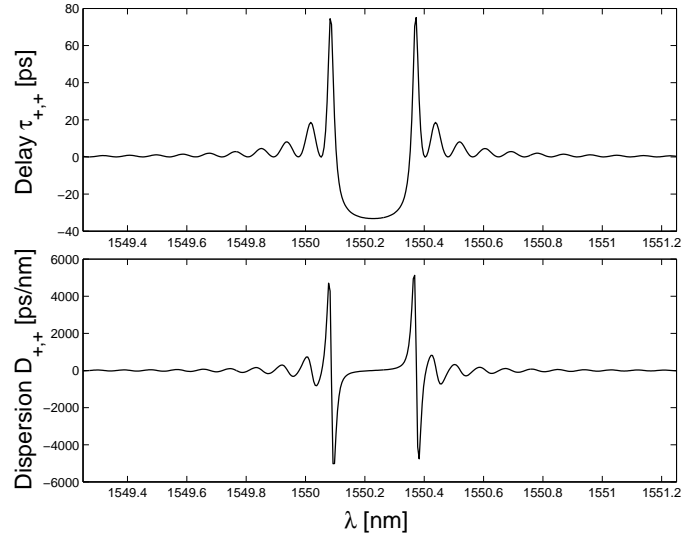


FIG. 12: Group delay and dispersion for the transmission coefficient of a uniform BG with $\kappa L = 4$. The corresponding spectrum is shown top right in Fig. 10

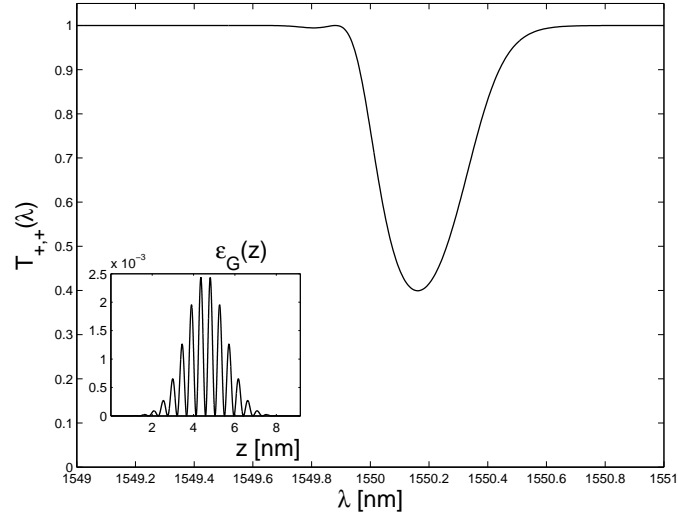


FIG. 13: Spectrum for a raised-Gaussian apodised BG. Insert: the raised-Gaussian dielectric modulation. The grating period has been exaggerated with respect to the length of the grating for clarity.

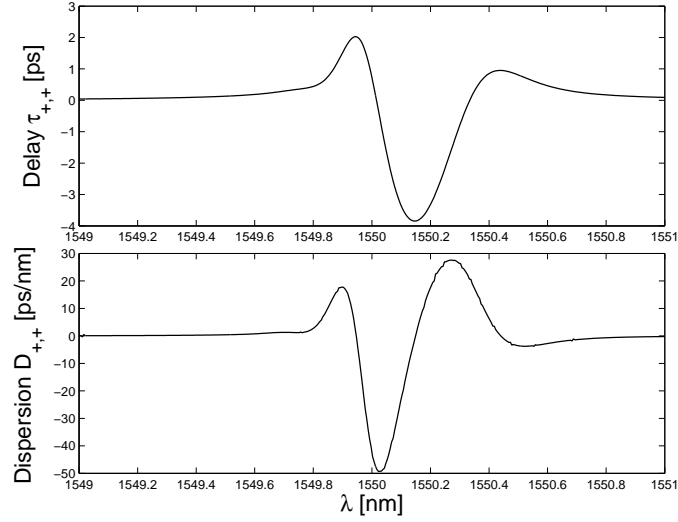


FIG. 14: Group delay and dispersion for a raised-Gaussian apodised BG. The spectrum of the grating is shown in Fig. 13.

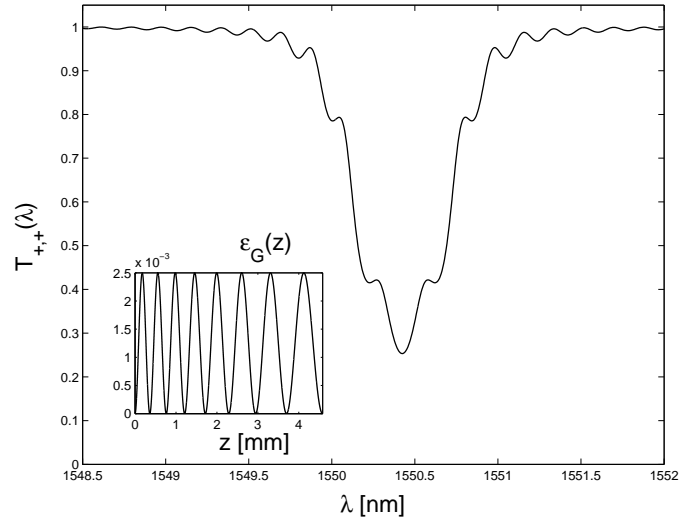


FIG. 15: Spectrum for a linearly chirped BG. Insert: the linearly chirped dielectric modulation. The chirp has been exaggerated with respect to the period of the grating for clarity.

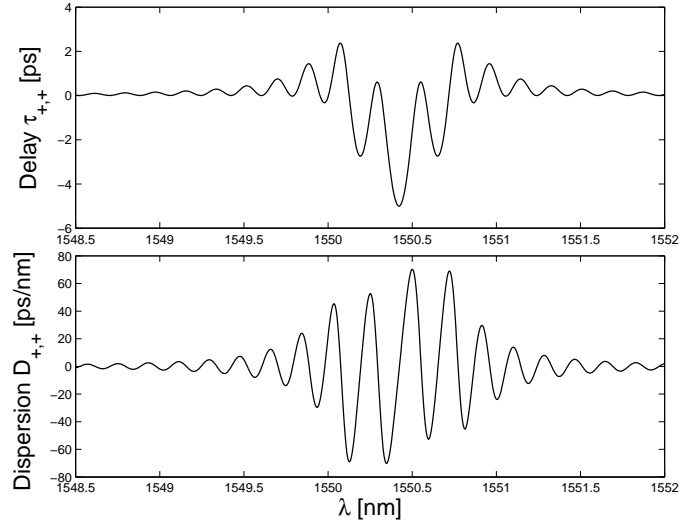


FIG. 16: Group delay and dispersion for a linearly chirped BG. The spectrum of the grating is shown in Fig. 15.